J Nanostruct 13(1): 92-103, Winter 2023

RESEARCH PAPER

Computational Investigation of the Electro-Optical and Thermal Characteristics of Ga Doped Graphene Molecule Structures

*Rajaa K. Mohammad [1], Sabeeh Jassim Gatea [2], Azhr Abdulzahraa Raheem [1], and Luma Majeed Ahmed [3]**

[1] *Department of Physics, College of Science, University of Kerbala, Karbala, Iraq*

[2] *Department of Physics, College of Science, University of Misan, Misan, Iraq*

[3] *Department of Chemistry, College of Science, University of Kerbala, Karbala, Iraq*

ARTICLE INFO

Article History:
Received 28 September 2022
Accepted 23 December 2022
Published 01 January 2023

Keywords:
Band gap
Fermi levels
Graphene Molecule
Optical properties
TD-DFT

ABSTRACT

This work is based on the density function theory (DFT) and time-dependent density function theory methods (TD-DFT) to investigate the density of states (DOS), FT-IR spectra, electro-optical and thermal, properties of Ga-doped Graphene molecule (GM). The Graphene molecule structure is found to be exhibiting semiconductor activity in a pure state with a wide band gap of 3.92301 eV. The defect of Graphene molecule with Ga has been demonstrated to depress the band gap values of GM structure significantly as a result of calculations. The electronic characteristics of graphene in its ground state and low-lying excited states may change based on the structural characteristics of Ga impurity in the GM structure. The results indicate that the electrical characteristics of GM are influenced by the geometrical distribution of Ga impurities in the GM structure. The consequences of Ga impurity are discussed for both GM ground and excited electronic states of GM are explored.

How to cite this article
Mohammad R K., Gatea S J., Raheem A A., and Ahmed L M. Computational Investigation of the Electro-Optical and Thermal Characteristics of Ga Doped Graphene Molecule Structures. J Nanostruct, 2023; 13(1):92-103. DOI: 10.22052/JNS.2023.01.011

INTRODUCTION

Graphite-like nano-platelets have attracted interest in composite materials as a viable and inexpensive filler [1, 2]. The design of new engineered nanomaterials for fuel cells, energy storage devices, biosensors, and gas sensors is favored using graphene, which has attracted great interest in the fields of composite materials and solid-state electronics [3]. This behavior is brought about by its exceptional physicochemical characteristics, which include great chemical stability and outstanding electromechanical qualities [4]. The two-dimensional substance known as graphene, which is made of carbon atoms organized in a honeycomb pattern, is also transparent [5, conducting [6, and bendable [7]. The fascinating electrical, optical, and mechanical characteristics of physics, chemistry, and materials science fields have sparked tremendous interdisciplinary interest [7]. Therefore, it is not surprising that graphene-based electronics are promising for future applications. In addition to the high technical potential, the relativistic nature of graphene charge carriers offers the opportunity to resolve the fundamental questions in condensed matter physics that are not accessible in any other material physics [8]. Graphene is regarded as one of the most important two-dimensional honeycomb

* *Corresponding Author Email: luma.ahmed@uokerbala.edu.iq*

This work is licensed under the Creative Commons Attribution 4.0 International License.
To view a copy of this license, visit http://creativecommons.org/licenses/by/4.0/.

structures that have been extensively studied in the last few years because of its possible mechanical and outstanding electronic applications and properties [9, 10]. Due to its exceptional sensitivity, which is beyond its high electron mobility, hence, graphene is a hard candidate employing as a gas sensor [11].

Experimentally [12] multiple studies of carbon atom replacement by impurities in various positions have been able to adjust graphene band structure calculations [13, 14]. The Ga, Ge, As, and Se substitutional doping of graphene is also researched for its effects. One could argue that the diversity and concentration of the dopant allow for the modification of the interaction. Doping opens a band gap in monolayer graphene generally. Ga doping, at certain doses, causes a half-metallic characteristic [15]. Utilizing first-principles calculations of electrical and structural property density values for states DOS and IR [16], the study of Nitrogen-Graphene's (N-G) sensitivity to several kinds of tiny gas molecules (CO, CO_2, OH, and B_2) had been estimated.

Given the foregoing, the goal of this work was to use the functional DFT/ B3LYP and the 3-21G basis to investigate the effects of doped Ga atoms in various places on the electrical, thermal, and optical properties for Graphene molecules. Where 3-21G basis set is more important because it splits and calculates both the valence electrons (which are the orbitals away from the active nucleus and responsible for the bonding) from the core electrons. In addition, the interactions of dispersion are not taken into account in this study.

COMPUTATIONAL APPROACH

Utilizing the software Gaussian 09 and Gaussian view 5.08 [17] and DFT, TD-DFT functional with B3LYP, Lee, Yang, and Parr's and 3-21G basis set [18], all computational procedure have been carried out. The electronic properties of GM, total energies (Et), highest occupied molecular orbital (HOMO), (E_{HOMO}), Fermi level energies (E_f), lowest unoccupied molecular orbital (LUMO) energies (E_{LUMO}), bandgap energies (E_g), and binding energies (Eb) were theoretically examined and analyzed for GM before and after replacement C atoms with Ga impurity in three different sites. By using (TD-DFT) calculation, at the excited states the electronic structure and excitation energies were found and estimated. In the gas phase and DFT method, the optical properties containing the excitation energy (E_{ex}), maximum absorption wavelengths (λ_{max}), and

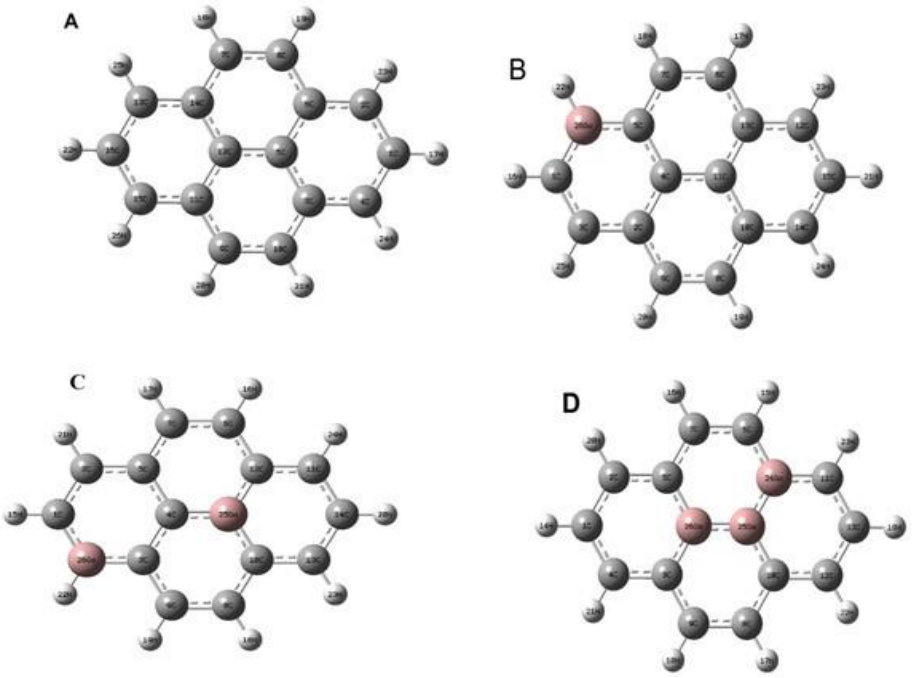

Fig. 1. The optimized structures of GM (A), GM +Ga(1)(B), GM + Ga(2) (C),and GM + Ga(3) (D) molecules using DFT method with3-21G basis set. Electronic properties.

CC BY

the optical bandgap (E_{og}) for GM +Ga were then performed at the B3LYP/3-21G level. The energy gap was computed using the Ionization potential (I) and electron affinity (E) equations and substituted their data in equation 1 [19]:

$$E_{gap} = E_{LUMO} - E_{HOMO} \quad (1)$$

$$I = -E_{HOMO} \quad (2)$$

$$E = E_{LUMO} \quad (3)$$

The Fermi energy (E_f) has been calculated using equation 4, which mention in reference [16]:

$$Ef = \left(\frac{EHOMO + ELUMO}{2}\right) \quad (4)$$

RESULTS AND DISCUSSION

Superior Structural

In accordance with the atomic numbering scheme indicated in Fig. 1, the optimal structural characteristics of molecules were estimated using DFT B3LYP levels with the 3-21G basis set. The bond lengths of C–H and C–C in Fig. 1 (A) are 1.0839 Å and 1.3942 Å respectively, but the bond lengths of C–H, C–C are increased to a range of 1.0866 Å and 1.4484 Å, respectively, when Ga atom is replaced in place of the C atom. In addition, with bond lengths equal to 1.9077 Å and 1.574 Å for GM +Ga(1) in Fig. 1(B), new bonds such as C–Ga, and Ga–H are made. On the other hand, with 1.0 909 Å, 1.4694 Å, 1.8138 Å, and 1.5767 Å for GM + Ga(2) in Fig. 1(C), and 1.0779 Å, 1.3914 Å, 1.8509 Å and 2.3881 for GM+ Ga(3) in Fig. 1(D), the same effect is obtained for the bond lengths of C–H and C–C,C–Ga, and Ga–H. The substitution of metal such as (Ga on graphene) would raise the electronic density and act as donor electrons to increase the length of the bond [20].

Electronic Properties

For GM (A), GM +Ga(1)(B), GM + Ga(2) (C), and GM + Ga(3) (D) molecules, the values of electronic properties such as HOMO, LUMO energies and electronic properties like (I, E, E_g, E_f and ET) were determined using DFT method with 3-21G basis set. In Table 1, these characteristics are summarized, before and after the addition of Ga as impurities, the energy gap, total energy, binding energy, HOMO, Fermi level, LUMO, and bandgap for GM.

Referring to Fig. 2, when Ga is substituted in various graphene positions as Fig. 1, the LUMO decreases, and the HOMO increases and decreases the band gap. The less value of bad gaps is found at GM + Ga(2) (C) and GM + Ga(3) (D) structures, which leads to an increase in the number of trap levels with an increase in the defect and increase the delocalization of the electrons by raising the number of Ga atoms in the structure of graphene. This situation will cause a red wavelength shift and reduce the band gap [21].

On the basis of the results achieved from table 1, the electron affinity (E) raises when Ga is substituted in various graphene positions as shown in Fig. 1. On the contrary, the ionization potential (I), the values of total energy (ET), Fermi level (Ef), and binding energy (Eb) depression values, will increase the electrical conductivity and make for a promising candidate to serve as an efficient way to the engineering of the electronic properties and stability of the GM, which can beemployed in semiconductor applications.

The Density of States

Fig. 3 depicts the relationship between the GM density of states (DOS) and energy level. DOS of the optimized indicated that the GM is a semiconductor with Eg ranging from (1.707762-3.92301) eV. There are many main peaks in all DOS. A high DOS at a particular energy level means that numerous states are occupyable. No

Table 1. HOMO, LUMO energies and electronic properties (I, E, Eg, Ef and ET) in (eV) units graphene before and after substituted by Ga.

Molecules	HOMO	LOUMO	I	E	Eg	Ef	ET	Eb
GM	-5.45771	-1.5347	5.45771	1.5347	3.92301	-1.9615	-612.379	-1051.42
GM +Ga(1)	-4.80329	-1.29443	4.803286	1.294427	3.508858	-3.04886	-2489.94	-1123.64
GM +Ga(2)	-5.24111	-3.41308	5.241111	3.413076	1.828035	-4.32709	-4367.41	-1195.85
GM +Ga(3)	-4.63349	-2.92573	4.633489	2.925727	1.707762	-3.77961	-6245.01	-1268.06

CC BY

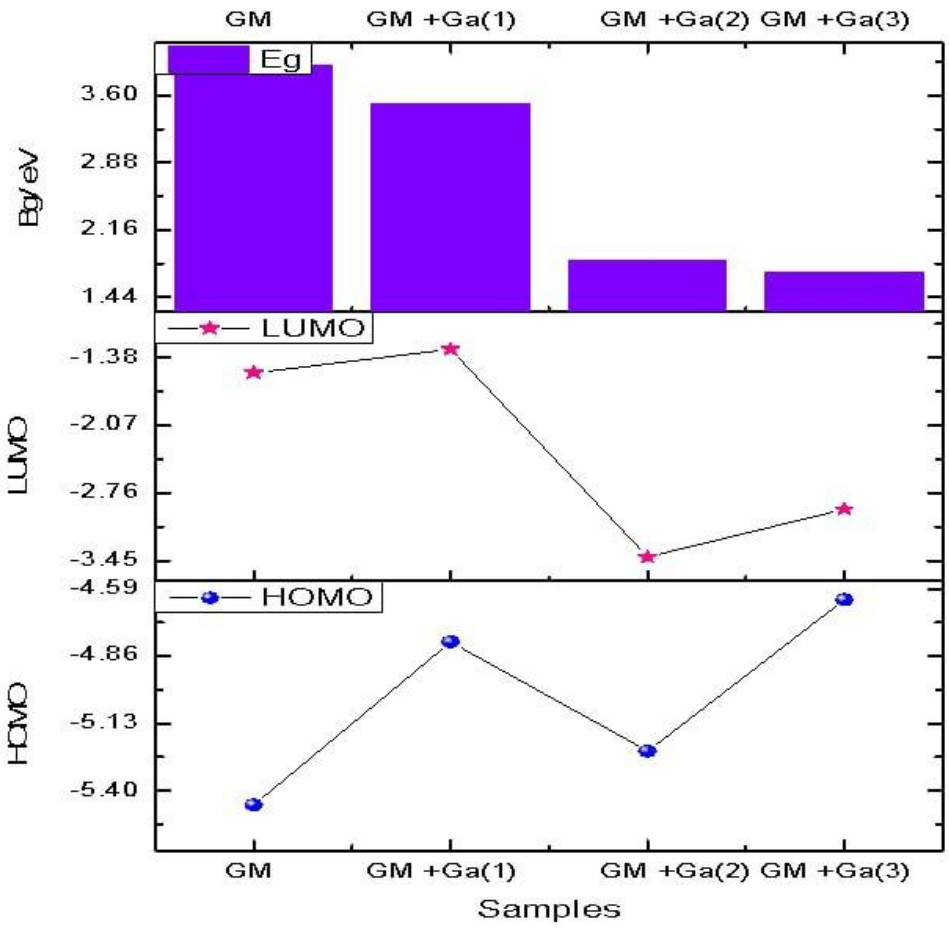

Fig. 2. Relationship of the (a) B_g, (b) HOMO, and (c) LUMO with graphene before and after substituted by Ga.

states can be filled at that energy level, which is shown by a zero-density of states. The DOS value for GM is (2.9044) from Fig. 3, the DOS values for the molecule under study were found to be higher than the DOS value for GM, and the DOS value for GM + Ga(2) was also higher than the DOS value for molecule under study. That due to the electronic charge is being dispersed between two substituted Ga atoms along the bond length. The main deduce in Fig. 3, changes in the electronic structure are observed by the DOS values depending on the positions of the Gaimpurity atom. So, the largest number of degenerate states in the conduction and valence bands is illustrated by GM +Ga(1), GM + Ga(2), and GM + Ga(3).

Optical Properties

For GM, the excitation energy (Eex), maximum absorption wavelengths (max), electronic transition assignments (O.S. (f)), and optical bandgap (Eog) have all been computed both before and after the Ga defect has been replaced with carbon atoms.

Table 2 illustrates that GM pure excitation energy has a value of 3.6117 eV, but reduces the excitation energy values to 1.561,2.1949 and 1.152 eV for GM +Ga(1), GM + Ga(2), and GM + Ga(3) configurations after replacing Carbon atoms with Ga impurity. Moreover, the result in table 2 and Fig. 4 indicated, that the maximum absorption wavelength of GM is raised as a red-shifted after Ga doping, and the maximum value occurs as the site of Ga impurity in GM structure. In this case, the optical bandgap (Eog), which is calculated by equation 5 [22, 23] and the electronic transition assignments (O.S (f)) are reduced, but the dipole moment for GM is increased.

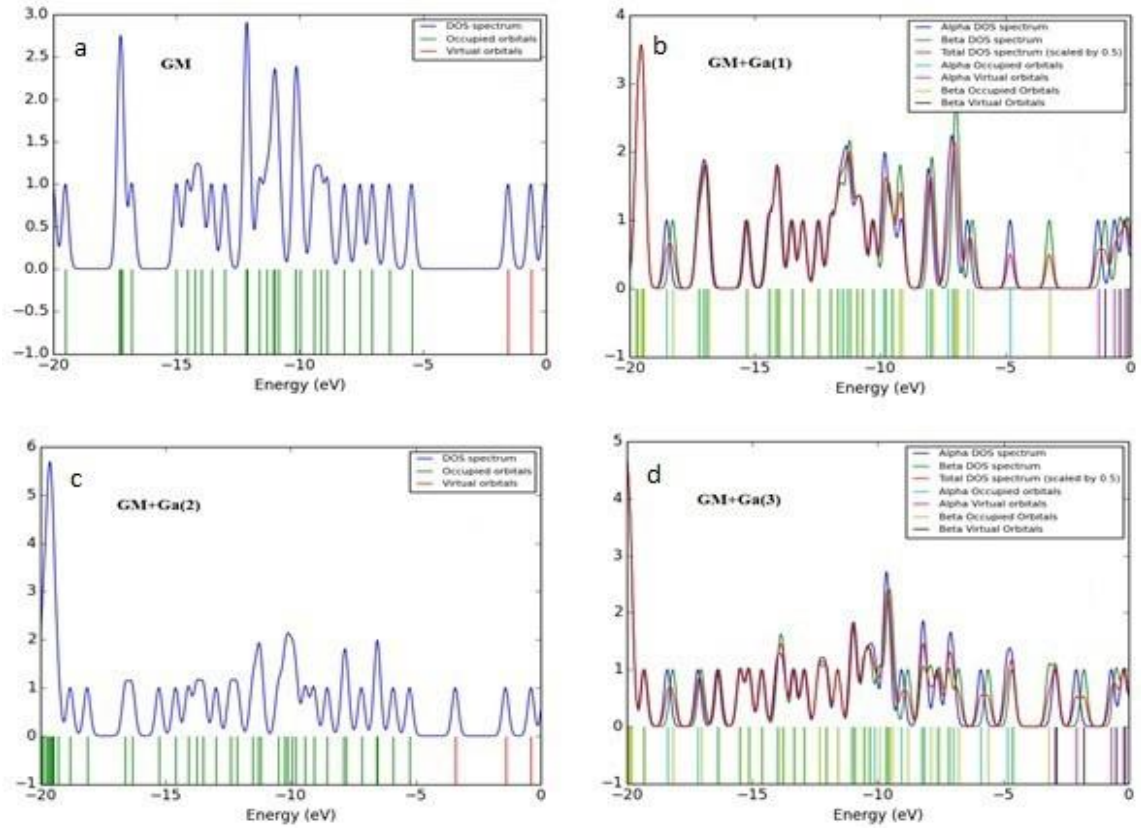

Fig. 3. The DOS of (a) GM , (b) GM +Ga(1) , (c) GM + Ga(2),and (d) GM + Ga(3) molecules using DFT method with 3-21G basis set.

Table 2. The measured electronic transition of systems, excitation energy (Eex), maximum absorption wavelengths (_ max), electronic transition assignments (O.S (f)), optical bandgap (Eog), and dipole moment (_, Debye),for GM before and after replacing C atoms with Ga impurity, for GM (A), GM +Ga(1)(B), GM + Ga(2) (C), and GM + Ga(3) (D) using DFT method with3-21G basis set.

Molecules	Eex	λmax	Eog	O.S (f)	(μ)
GM	3.6117	343.29	3.58124	0.3255	0
GM +Ga(1)	1.561	794.26	3.80573	0.006	1.994
GM +Ga(2)	2.1949	564.88	2.865318	0.0001	1.0136
GM +Ga(3)	1.1512	1077.01	1.703409	0.0002	I.0764

$$E_{og} = \frac{1240}{\lambda_{max}} \quad (5)$$

As it is clear in Fig. 4, the substitution of Ga on GM causes to shift in the peak of GM toward long wavelength with decreases in the bandgap, excitation energy, and electronic transition assignments, that due to the d-d orbital of metal. Moreover, there are two peaks that occur in the GM + Ga(3) in the (D) spectrum that correspond to a high number of substituted Ga, so one of the peaks is high intensity and shifted compared with the other substituted Ga in another spectrum, that attitude to concert the d-d orbitals for three

CC BY

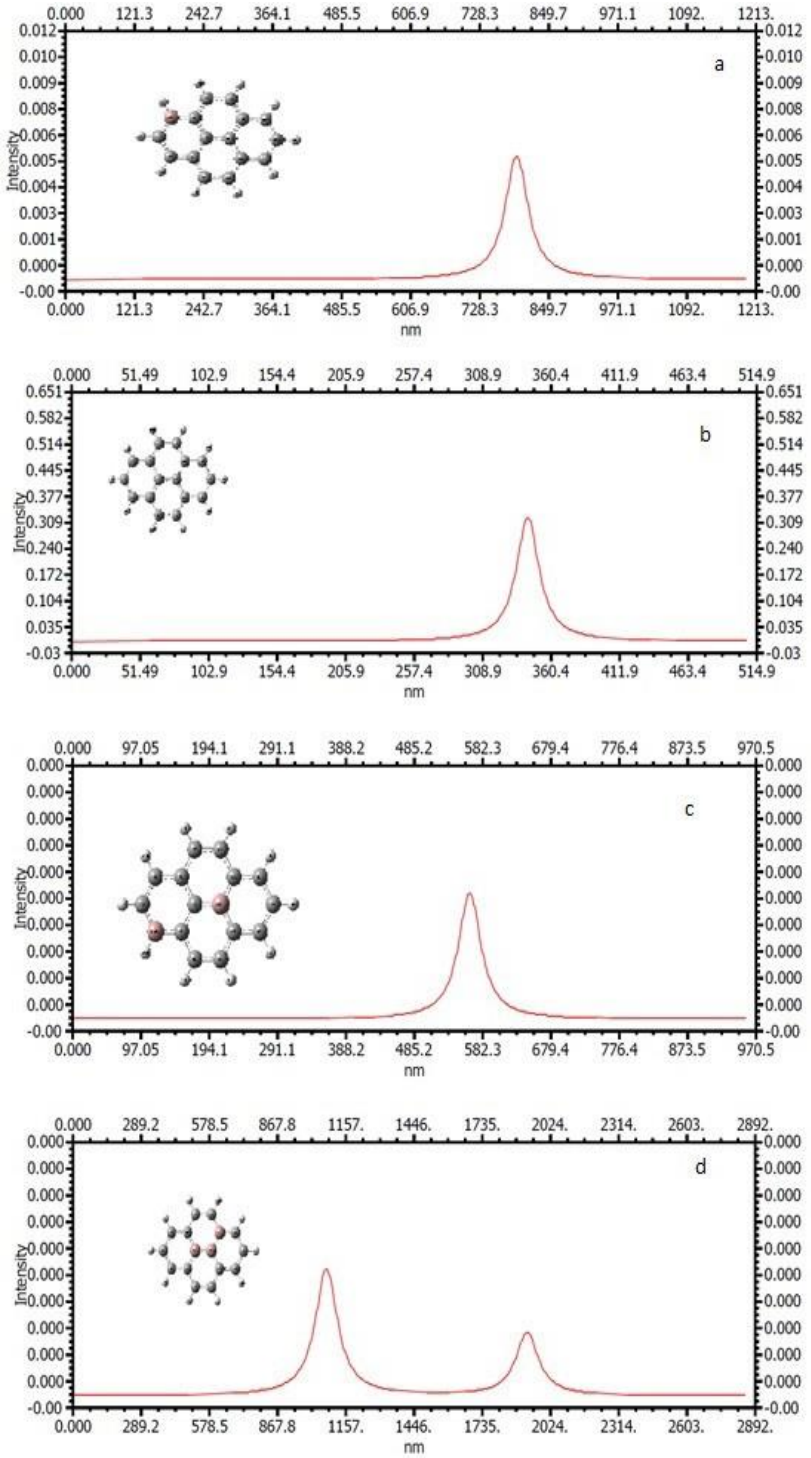

Fig. 4. Absorption spectra of (a) GM , (b) GM +Ga(1), (c) GM + Ga(2),and (d) GM + Ga(3) molecules using DFT method with 3-21G basis set.

atoms of Ga in small position on GM structure. On the other side, the substitution of Ga on GM leads to generating a dipole moment on the GM surface, but concentrating the Ga atoms in a small position of GM leads to reducing the dipole moment value that depended on the nature of the Ga atom. The

CC BY

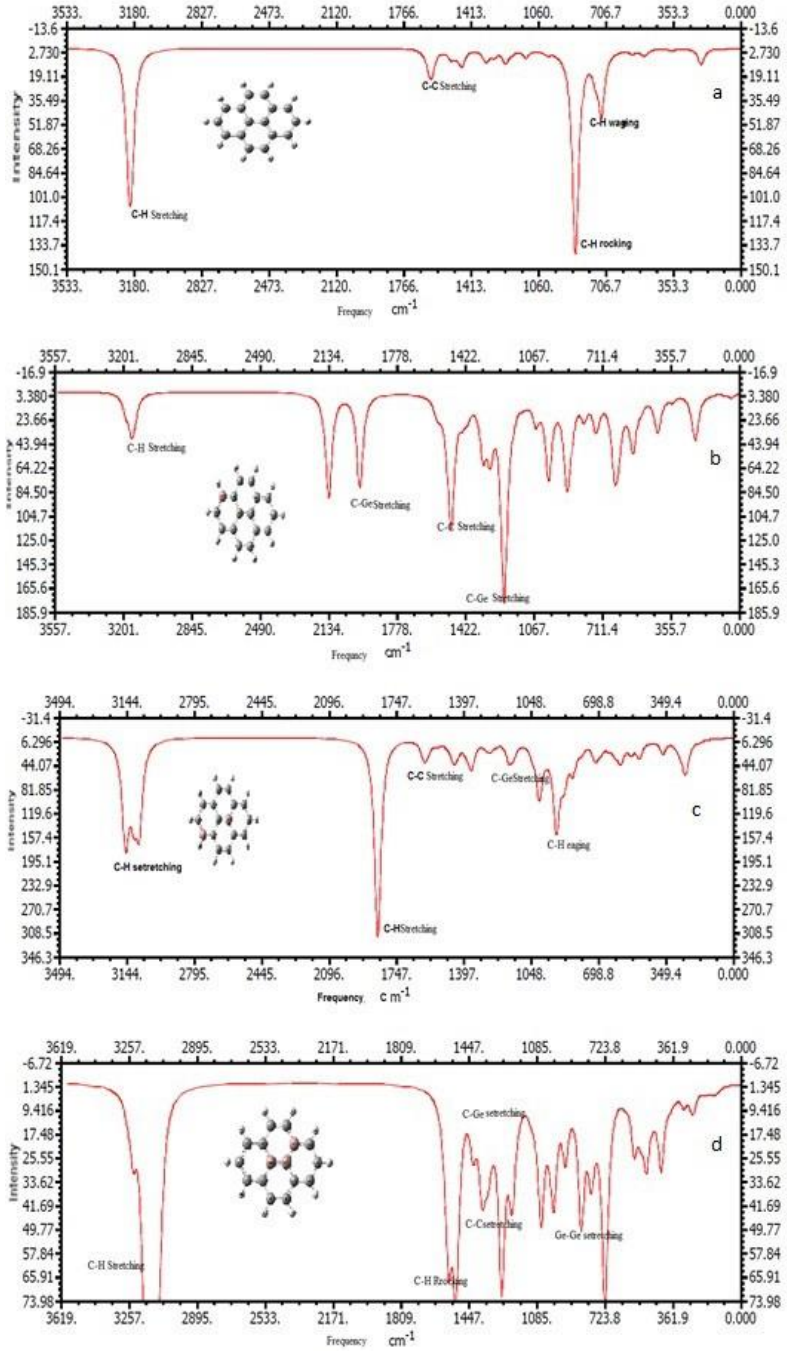

Fig. 5. FTIR spectra of (a) GM , (b) GM +Ga(1), (c) GM + Ga(2), and (d) GM + Ga(3) molecules using DFT method with 3-21G basis set.

band gap of GM increases with the substitution of Ga which will cause an increase in the number of internal levels that make the Bg is small also the Ga work as a sink of an electron that increases the separation between the charge and raises the semiconductor activity.

FTIR Spectra

In the region 3212.65 cm^{-1},1625.10 cm^{-1},1545.38 cm^{-1} and 767.273 cm^{-1} waging, the FTIR spectra of

CC BY

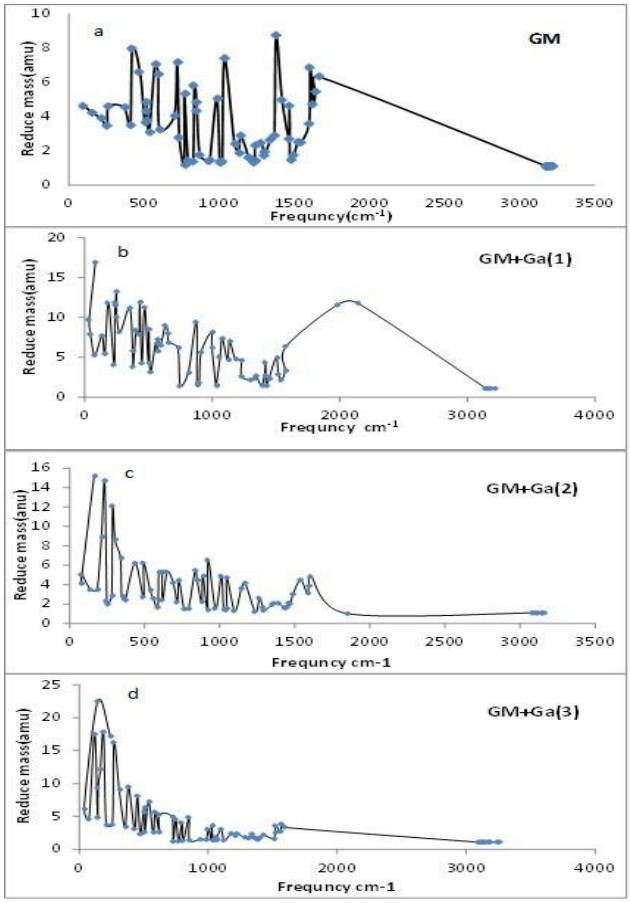

Fig. 6. The reduce mass of (a) GM , (b) GM +Ga(1), (c) GM + Ga(2),and (d) GM + Ga(3) molecules using DFT method with 3-21G basis set.

the C-H, C–C, stretching C-H rocking and C–H waging exam- ined are weak for GM, as indicated in Fig. 5, the C–H,C–C, and C–Ga stretching for GM + Ga(1), GM + Ga(2), and GM + Ga(3) in the reign 1847.7- 3278.8 cm^{-1} C–H stretching, the C-C stretching examined in the region 1277.99 -1608.56 cm^{-1} and C–Ga stretching studied in the region1169.06-1318.82 cm^{-1} . The GM + Ga(3) 768.409 cm^{-1} Ga–Ga stretching mode, as presented in Fig. 5.

The impurities contribute to increasing the

Table 3. Eth, CV and S in Kcal/mol and cal/mol-Kelvin units for GM , GM+Ga(1) GM + Ga(2),and GM + Ga(3) molecules using DFT method with3-21G basis set.

Molecules	Eth	CV	S
GM	137.115	43.858	94.147
GM +Ga(1)	131.214	48.638	106.744
GM +Ga(2)	125.037	53.438	113.284
GM +Ga(3)	125.152	53.655	119.849

(cc) BY

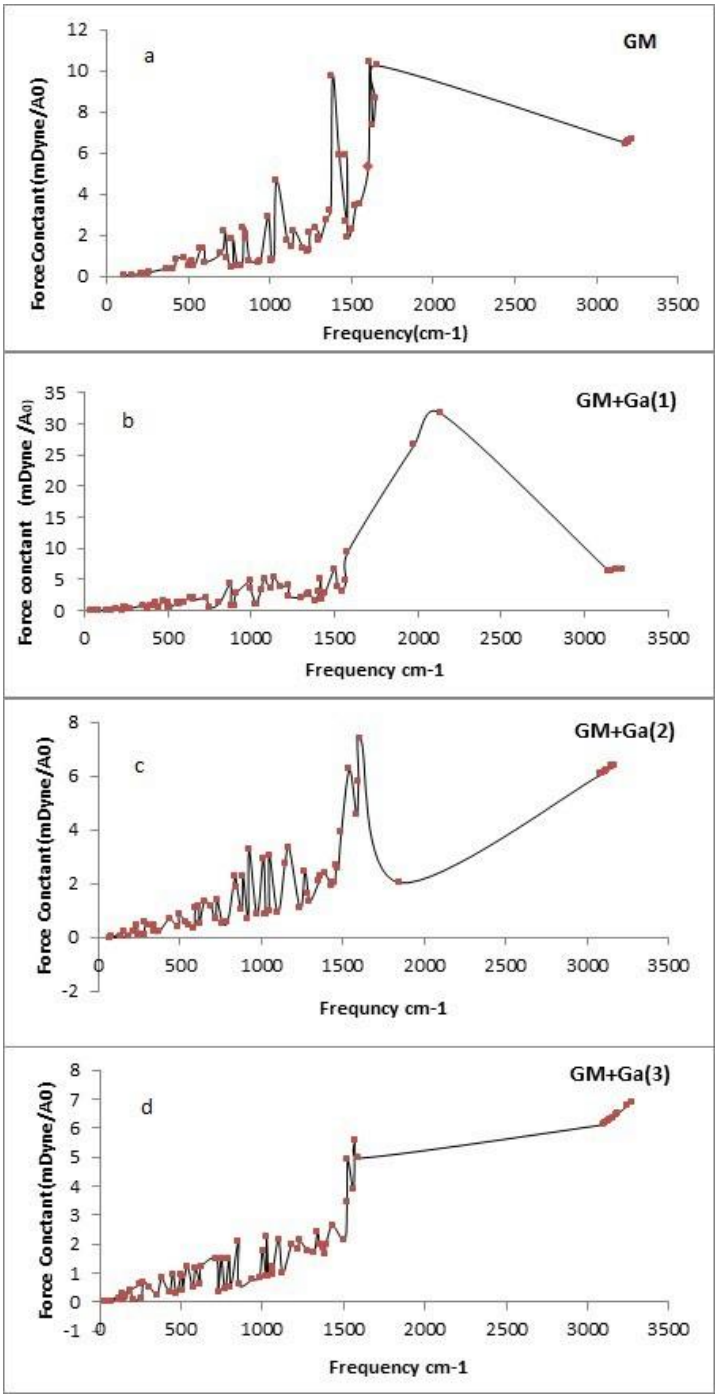

Fig. 7. The force constant of (a) GM , (b) GM +Ga(1), (c) GM + Ga(2),and (d) GM + Ga(3) molecules using DFT method with 3-21G basis set.

vibration modes for the understudy GNRS. In region 309.68 cm^{-1} and 188.302 cm^{-1} region, The GM + Ga(3) has C–H waging and Ga–Ga rocking is weak. From this figure, the effect of Ga atoms can be seen, leading to weak vibration harmonic [24, 25].

Force Constant and Reduced Masses

For the purpose of comprehending vibrational modes, the quantity, decreased mass, and force-constant of each atom in the structures are computed. Fig. 6 and Fig. 7 were used to estimate the force constant and reduce mass, and the optimized structures of GM, GM +Ga(1) GM + Ga(2) and GM + Ga(3) molecules were detected using the DFT method with a 3-21G basis set. In Fig. 6, the GM +Ga(3) has highest reduce mass at 31.8096 a.u. The reduced mass for all GM is reduced from these estimates which indicates that certain vibration could involve one from of atom and exclude the other, while the constant force is rising. The rationale for these results is inversely proportional to frequency due to the lower mass, although equation 6's mention [26, 27] of the force constant (k) indicates that it is directly proportional to frequency (v).

$$v = 1/2\pi\sqrt{k/\mu} \quad (6)$$

Fig. 7 is divided into two regions depending on the force constant with a value of reduced mass, first region range begins from 0 to 1585.8 cm^{-1}. The second region range is started from 1450 cm^{-1} to near 3500 cm^{-1}. The GM + Ga(3) has the maximum force constant at 22.4949 m $Dyne/\mathring{A}$.

Thermal Characteristics

Table 3 and Fig. 8 show that the calculated values of the thermal properties (Eth, C_v and S) using DFT method with B3LYP. After the substitution of Ga in GM, the entropy increases and reaches the maximum value with more than two Ga atoms substituted, so the maximum entropy value is obtained in GM+Ga(3) sample that, due to a random rise in the graphene structure. The C_v and Eth decrease with Ga doped at the same time, that attitude increases the stability of GM with defect by Ga.

Electrostatic potential and electron density surfaces (ESP)

The Electrostatic potential and electron density surfaces for GM, GM +Ga(1) GM+ Ga(2) and GM + Ga(3) are computed from DFT method with 3-21G basis set as shown in 9. The type of substitution atoms, as well as negative and positive charges, affect how electrostatic potential and electron density surfaces are distributed. From this figure, the density distribution on GM is homogeneous, GM

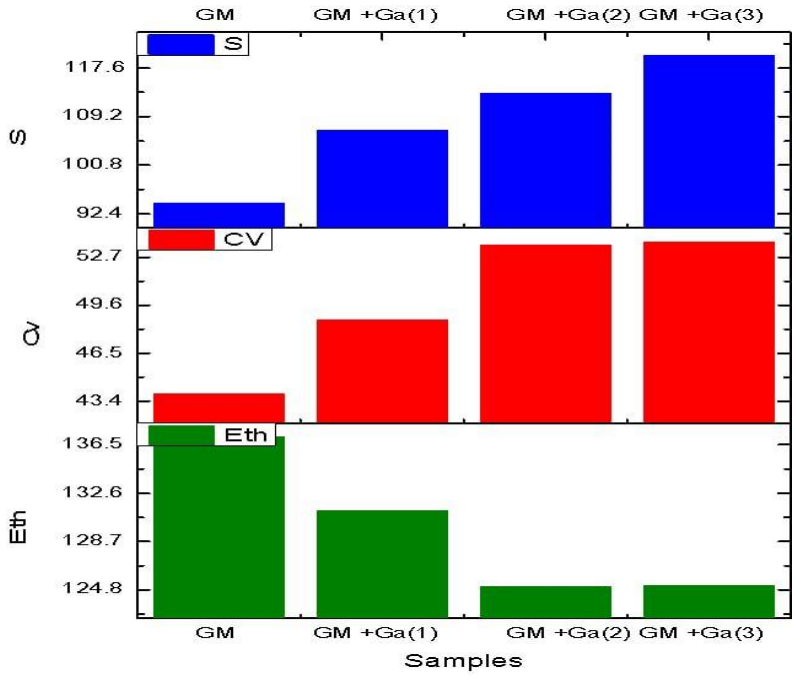

Fig. 8. Relationship of the (a) S, (b) C_v and (c) Eth with CNTS before and after substituted by halogens.

CC BY

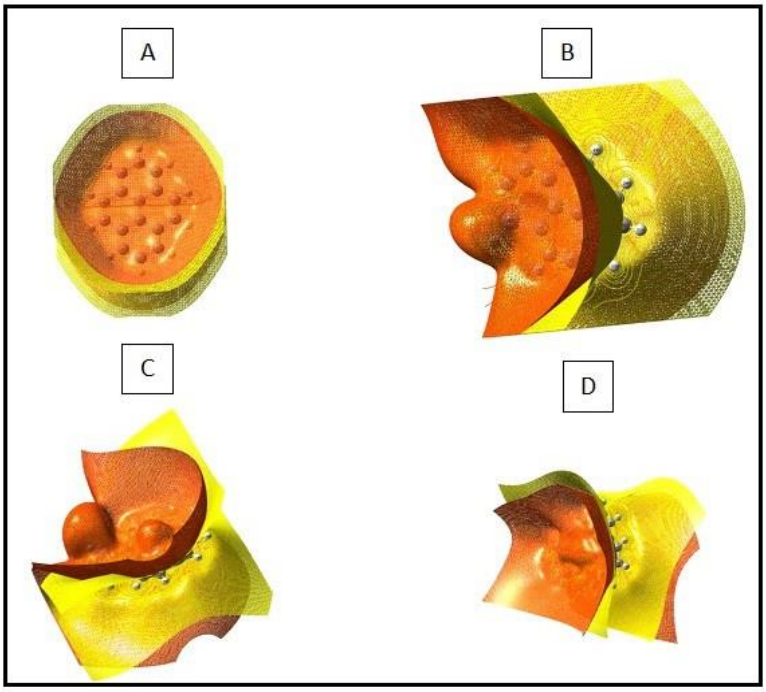

Fig. 9. The electrostatic potential and electron density surfaces for GM (A), GM +Ga(1) (B), GM+Ga(2) (C), and GM + Ga(3) (D) are computed for DFT method with3-21G basis set.

+Ga(1), GM + Ga(2), and GM + Ga(3) molecules distribution on the Ga atoms. Because of their great electro negative, these atoms draw charge to themselves.

CONCLUSION

In this paper, the electronic properties of GM, total energies (Et), highest occupied molecular orbital (HOMO), (E_{HOMO}), Fermi level energies (Ef), lowest unoccupied molecular orbital (LUMO) energies (E_{LUMO}), bandgap energies (Eg), and binding energies (Eb) were measured and theoretically analyzed for GM before and after replacement of C atoms with Ga impurity in three varies sites. And TD-DFT to discover the optical properties. The values of HOMO, Fermi level, and binding energy total energy are increasing, while, the values of total energy, ionization potential I, LUMO, electron affinity E, and band gap Eg are decreasing but when subtitled of Ga. The Eg (1.7077 eV) of GM + Ga(3) indicates a semiconductor character. The GM +Ga(1) has a high Eg of molecules under study. The pure GM has a maximum bandgap energy value compared with the value for the structure before Ga impurity. GM pure excitation energy has 3.6117 eV, but after replacing C atoms with Ga impurity, the excitation energy values for configuration of GM + Ga(1), GM + Ga(2) and GM + Ga(3) are 1.561, 2.1949 and 1.152 eV respectively. This result demonstrates that the excitation energies of GM are red-shifted by the defect. The maximum absorption wavelength alters from 343.29 nm for the pure GM to 794.26 nm for structure GM with one Ga GM , GM +Ga(1) GM + Ga(2), and GM + Ga(3) molecules using DFT method with 3-21G basis set. When impurity of GM with Ga(1), the effect of Ga atom in FTIR spectra leads to weak vibration harmonics. The changes in electronic structure are observed in DOS values, depending on the positions of Ga impurity atoms. In many applications, impurity is very important because electrical conductivity can be changed and leads to a small change in bandgap value.

ACKNOWLEDGMENTS

We are grateful to the Department of Physics, College of Science, University of Kerbala, for supporting this work.

CONFLICT OF INTEREST

The authors declare that there is no conflict of interests regarding the publication of this manuscript.

REFERENCES

1. Drzal PL, Barnes JD, Kofinas P. Path dependent microstructure orientation during strain compression of semicrystalline block copolymers. Polymer. 2001;42(13):5633-5642.
2. Kalaitzidou K, Fukushima H, Drzal LT. Multifunctional polypropylene composites produced by incorporation of exfoliated graphite nanoplatelets. Carbon. 2007;45(7):1446-1452.
3. Qi Y, Zhang Y, Liu C, Zhang T, Zhang B, Wang L, et al. A tunable terahertz metamaterial absorber composed of elliptical ring graphene arrays with refractive index sensing application. Results in Physics. 2020;16:103012.
4. Pumera M, Ambrosi A, Bonanni A, Chng ELK, Poh HL. Graphene for electrochemical sensing and biosensing. TrAC, Trends Anal Chem. 2010;29(9):954-965.
5. Nair RR, Blake P, Grigorenko AN, Novoselov KS, Booth TJ, Stauber T, et al. Fine Structure Constant Defines Visual Transparency of Graphene. Science. 2008;320(5881):1308-1308.
6. Lee C, Wei X, Kysar JW, Hone J. Measurement of the Elastic Properties and Intrinsic Strength of Monolayer Graphene. Science. 2008;321(5887):385-388.
7. Geim AK. Graphene: Status and Prospects. Science. 2009;324(5934):1530-1534.
8. Peres NMR. Graphene, new physics in two dimensions. Europhysics News. 2009;40(3):17-20.
9. Wu C-S, Chai J-D. Electronic Properties of Zigzag Graphene Nanoribbons Studied by TAO-DFT. J Chem Theory Comput. 2015;11(5):2003-2011.
10. Castro Neto AH, Guinea F, Peres NMR, Novoselov KS, Geim AK. The electronic properties of graphene. Rev Mod Phys. 2009;81(1):109-162.
11. Luan VH, Han JH, Kang HW, Lee W. Ultra-sensitive non-enzymatic amperometric glucose sensors based on silver nanowire/graphene hybrid three-dimensional nanostructures. Results in Physics. 2019;15:102761.
12. Rad AS, Kashani OR. Adsorption of acetyl halide molecules on the surface of pristine and Al-doped graphene: Ab initio study. Appl Surf Sci. 2015;355:233-241.
13. Rad AS. Al-doped graphene as modified nanostructure sensor for some ether molecules: Ab-initio study. Synth Met. 2015;209:419-425.
14. Mohammad R, Jassim S, Ahmed L. Halogens Substitution Effects on Electronic and Spectral Properties of Carbon Nanotube Molecules studying with the DFT method. Egyptian Journal of Chemistry. 2021;0(0):0-0.
15. Denis PA. Chemical Reactivity and Band-Gap Opening of Graphene Doped with Gallium, Germanium, Arsenic, and Selenium Atoms. Chemphyschem. 2014;15(18):3994-4000.
16. Parey V, Jyothirmai MV, Kumar EM, Saha B, Gaur NK, Thapa R. Homonuclear B2/B3 doped carbon allotropes as a universal gas sensor: Possibility of CO oxidation and CO2 hydrogenation. Carbon. 2019;143:38-50.
17. Hilfiker R. Wissenschaft erklärt: Aufbau wissenschaftlicher Artikel – Immer dasselbe! ergopraxis. 2009;02(09):17-17.
18. Petersson GA, Al-Laham MA. A complete basis set model chemistry. II. Open-shell systems and the total energies of the first-row atoms. The Journal of Chemical Physics. 1991;94(9):6081-6090.
19. Mohammad RK, Mohammad MR, Ahmed DS. Ab initio study of the solvent effects on the electronic and vibrational properties of formic acid molecules. AIP Conf Proc: AIP Publishing; 2019.
20. Kaufman GB. Inorganic chemistry: principles of structure and reactivity, 4th ed. (Huheey, James E.; Keiter, Ellen A.; Keiter, Richard L.). J Chem Educ. 1993;70(10):A279.
21. Ahmed LM, Ivanova I, Hussein FH, Bahnemann DW. Role of Platinum Deposited on TiO_2 in Photocatalytic Methanol Oxidation and Dehydrogenation Reactions. International Journal of Photoenergy. 2014;2014:1-9.
22. Grimme S, Hujo W, Kirchner B. Performance of dispersion-corrected density functional theory for the interactions in ionic liquids. Physical Chemistry Chemical Physics. 2012;14(14):4875.
23. Indriani D, Fahyuan HD, Ngatijo N. UJI. uv-vis lapisan TiO_2/N_2 untuk menentukan band gap energy. Journal online of physics. 2018;3(2):6-10.
24. Malaescu D, Grozescu I, Sfirloaga P, Vlazan P, Marin CN. The Electrical Properties of Some Composite Materials Based on Sodium and Tantalum Oxides. Acta Phys Pol, A. 2016;129(1):133-137.
25. Nakamoto K. Infrared and Raman Spectra of Inorganic and Coordination Compounds: Wiley; 2008 2008/04/30.
26. Brisdon A. Kazuo Nakamoto Infrared and Raman Spectra of Inorganic and Coordination Compounds, Part B, Applications in Coordination, Organometallic, and Bioinorganic Chemistry, 6th edn Wiley, 2009, 424 pp. (hardback) ISBN 978-0-471-74493-1. Appl Organomet Chem. 2010:n/a-n/a.
27. MacDougall, Frank H. Physical chemistry. New York: The Macmillan Company, 1952. 750 P. $6.00. Science Education. 1954;38(4):320-320.